nature plants

ARTICLES

PUBLISHED: 27 MAY 2016 | ARTICLE NUMBER: 16072 | DOI: 10.1038/NPLANTS.2016.72

Hydraulic basis for the evolution of photosynthetic productivity

Christine Scoffoni[1]*, David S. Chatelet[2,3], Jessica Pasquet-kok[1], Michael Rawls[1], Michael J. Donoghue[3], Erika J. Edwards[2] and Lawren Sack[1]

Clarifying the evolution and mechanisms for photosynthetic productivity is a key to both improving crops and understanding plant evolution and habitat distributions. Current theory recognizes a role for the hydraulics of water transport as a potential determinant of photosynthetic productivity based on comparative data across disparate species. However, there has never been rigorous support for the maintenance of this relationship during an evolutionary radiation. We tested this theory for 30 species of *Viburnum*, diverse in leaf shape and photosynthetic anatomy, grown in a common garden. We found strong support for a fundamental requirement for leaf hydraulic capacity (K_{leaf}) in determining photosynthetic capacity (A_{max}), as these traits diversified across this lineage in tight coordination, with their proportionality modulated by the climate experienced in the species' range. Variation in K_{leaf} arose from differences in venation architecture that influenced xylem and especially outside-xylem flow pathways. These findings substantiate an evolutionary basis for the coordination of hydraulic and photosynthetic physiology across species, and their co-dependence on climate, establishing a fundamental role for water transport in the evolution of the photosynthetic rate.

The field of water relations is crucial to understanding plant growth and function. Over the past 400 million years, plant water transport has undergone drastic evolutionary changes, from direct absorption of water into cells by osmosis in mosses and liverworts to the evolution of a wide range of vascular anatomies that enable rapid transport in several lineages of 'non-vascular' plants and commonly across the vascular plants[1]. For the past 30 years, studies have hypothesized that the evolution of a more efficient water transport system has enabled the diversification of photosynthetic capacity[2–4], allowing species to establish across diverse habitats, and past studies have shown coordination of water transport with photosynthesis across diverse lineages both physiologically (refs 5–8; reviewed in Supplementary Table 1), and anatomically[7,9,10]. However, evolutionary processes occur at smaller scales where species do not exhibit the extreme phenotypes observed across the entire evolutionary tree. Indeed, comparing trait coordination across highly disparate versus closely related species can give strongly opposing conclusions. The smaller variation in traits among closely related species could result in the disappearance or reversal of trends observed at larger scales, in which case it becomes impossible to argue that the ties between those variables are causal. To establish a truly evolutionary coordination or causality, tests must be made using closely related plants in well-resolved lineages in a common garden[11–16]. Even well-established trends across diverse species, such as the leaf economics spectrum, have been found to disappear when considered within lineages, showing that they are not necessarily causal as previously hypothesized[11,14,16,17]. Indeed, a recent study testing the linkage between light-saturated photosynthetic rate and leaf-area-based stem hydraulic conductance ($K_{stem,L}$) across 27 species of Magnoliaceae found no significant evolutionary correlation[18] (Supplementary Table 1). However, a strong test of theory would focus on the efficiency of water movement through the leaf (leaf hydraulic conductance; K_{leaf}), recognized as a bottleneck in the whole plant system[19] (Fig. 1). Our aim was to perform a strong test of the theory of hydraulic–photosynthetic coordination within the evolution of closely related species to address this issue and elucidate the mechanisms for leaf hydraulic evolution and its influence on plant productivity.

When leaves open their stomata to capture CO_2 for photosynthesis, water is transpired to the atmosphere, potentially dehydrating the leaf, and the ability of stomata to remain open for photosynthesis depends on the plant's capacity to replace that water. Consequently, hydraulic supply should match stomatal conductance (g_s). In drier and/or warmer climates, leaves would require an increased hydraulic supply to mitigate the greater evaporative loads. This would enable leaves to achieve a given g_s and thereby maintain adequate photosynthetic rates[20,21], given that g_s and A_{max} tend to be highly correlated[22,23]. A higher K_{leaf} could arise because of shifts in xylem and/or outside-xylem properties, and strongly influence the photosynthetic rate.

We synthesized current theory on the hydraulic basis for evolutionary shifts in gas exchange and climate niche (Supplementary Appendix 1), and we tested its predictions for the genus *Viburnum* (Adoxaceae), an emerging model lineage for examining the evolution of leaf form and function[16,24–27]. *Viburnum* consists of ~165 species from temperate and tropical forests with leaves that are exceptionally diverse in shape and photosynthetic anatomy[24,25]. We quantified K_{leaf}, g_s, A_{max} and their anatomical correlates in 30 *Viburnum* species originating from across the Northern Hemisphere and grown in a common garden, and tested hypothesized evolutionary correlations for the coordination of hydraulic efficiency, gas exchange and climate, and for the mechanisms of leaf hydraulic diversification. K_{leaf} represents the efficiency of water transport through a complex micro-hydrological system: water moves within xylem conduits through the petiole and throughout the leaf venation network, then across the bundle sheath and mesophyll cells to the sites of evaporation. Previous

[1]Department of Ecology and Evolutionary Biology, University of California Los Angeles, 621 Charles E. Young Drive South, Los Angeles, California 90095, USA. [2]Department of Ecology and Evolutionary Biology, Brown University, Box G-W, 80 Waterman St., Providence, Rhode Island 02912, USA. [3]Department of Ecology and Evolutionary Biology, Yale University, PO Box 208106, New Haven, Connecticut, 06520-8106, USA. *e-mail: cscoffoni@ucla.edu

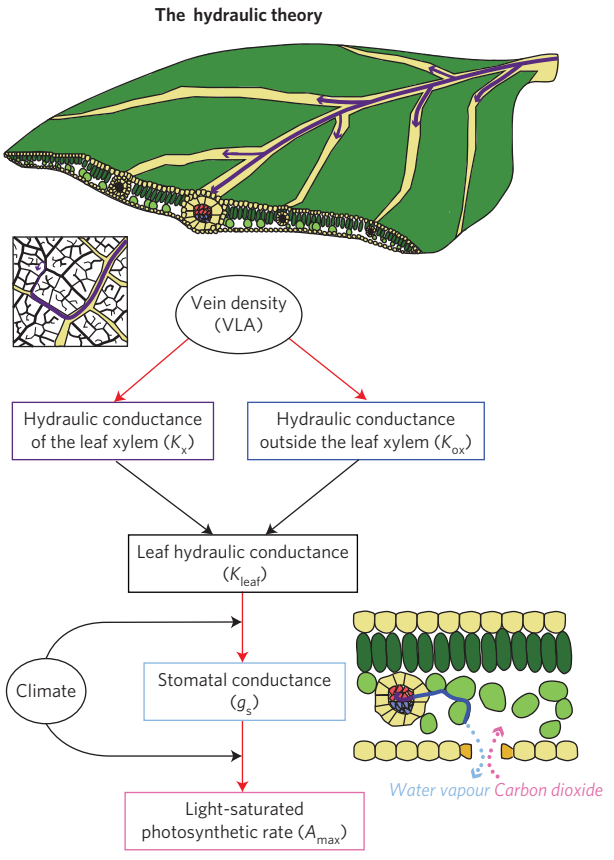

Figure 1 | Description of the hydraulic theory as a driver of leaf gas exchange. Leaf hydraulic conductance, which is composed of both xylem hydraulic conductance (purple) and outside-xylem conductance (dark blue; equation (1)), acts as a limitation on both stomatal conductance (light blue) and light-saturated CO_2 assimilation rate (pink) because it determines the efficiency with which transpired water is replaced, and therefore the degree that stomata can remain open to allow photosynthesis. Vein length contributes to both higher xylem and outside-xylem hydraulic conductances. Mesophyll anatomy and biochemistry (including aquaporin activity) also influences the outside-xylem conductance. Red arrows indicate a role for additional factors in the determination of hydraulics and gas exchange traits, including, e.g. xylem and mesophyll/bundle sheath anatomy, nitrogen content and other biochemical traits, stomatal and photosynthetic anatomy and the vapour pressure gradient. Climate modulates the K_{leaf}/g_s and K_{leaf}/A_{max} relationships (see theory derivation in Supplementary Appendix 1).

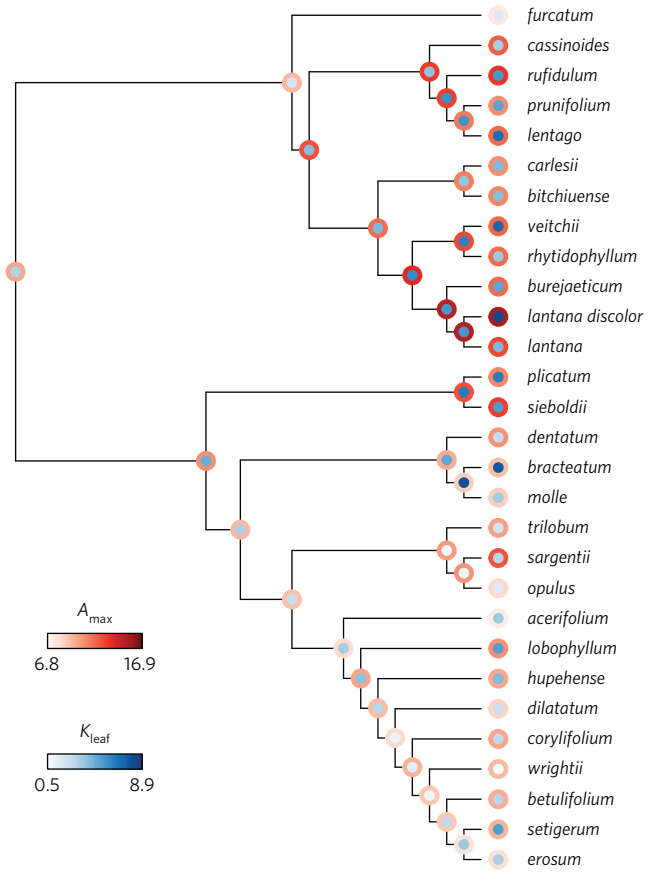

Figure 2 | Estimated ancestral states for K_{leaf} and A_{max} showing their co-evolution across the phylogenetic tree for *Viburnum* species. Tree reveals coordinated trait evolution not only at the tips of the tree but also for the inferred ancestral traits. Symbols: K_{leaf}, leaf hydraulic conductance at leaf water potential of −0.3 MPa, units are given in mmol m^{-2} s^{-1} MPa^{-1}; A_{max}, light-saturated CO_2 assimilation rate in μmol m^{-2} s^{-1}.

studies found that species vary greatly in the proportion of hydraulic resistance distributed in the xylem versus outside xylem pathways, with the percentage resistance outside the xylem (R_{ox}) varying from 11 to 88% across 14 tropical and temperate tree species[28–30]. For a diverse subset of 17 *Viburnum* species, we measured the hydraulic conductance of the pathways within and outside the xylem (K_x and K_{ox} respectively), where

$$K_{leaf} = (K_x^{-1} + K_{ox}^{-1})^{-1} \quad (1)$$

We analysed the relationship of K_x and K_{ox} to leaf vascular anatomy. Modeling and studies across a few disparate species have shown that K_x increases with more and/or larger vein xylem conduits[9,31] and both K_x and K_{ox} can increase with higher vein length per area (VLA) because of a greater number of parallel flow pathways through the vein network, a larger surface area for water to exit the veins, and shorter flow path lengths outside the xylem[9,32,33].

We tested the major propositions of plant hydraulic theory for the relationship of hydraulic, stomatal and photosynthetic physiology and their modulation by climate (Fig. 1 and Supplementary Appendix 1). In particular, we examined whether, during the evolutionary diversification of leaves in this lineage, (1) hydraulic supply matched demand, such that K_{leaf}, g_s and A_{max} evolved in coordination, with a higher K_{leaf} relative to g_s and A_{max} in warmer and drier climates[3,20,21]. We also tested the prediction that (2) evolutionary shifts in K_{leaf} would relate to shifts in venation architecture. Given that mesophyll tissue anatomy is so diverse across *Viburnum*[25], we hypothesized (3) that outside xylem pathways would be especially important in determining K_{leaf} diversification.

Results

We found 18-fold variation in K_{leaf} across *Viburnum* species, from 0.48 to 8.9 mmol m^{-2} s^{-1} MPa^{-1} (Supplementary Table 2; see Supplementary Material and Methods), far greater than the variation in the light-saturated CO_2 assimilation rate (A_{max}) and stomatal conductance (g_s), which varied by 2.5- and 3.3-fold respectively ($P < 0.001$ for each, analysis of variance (ANOVA), Supplementary Table 2). Across species, g_s and A_{max} evolved in tight coordination with shifts in K_{leaf}, with shifts up or downwards in gas exchange variables along branches of the phylogenetic tree corresponding to shifts in K_{leaf} (Figs 2 and 3). We found strong coordination of nitrogen per leaf area (N_{area}) with A_{max} and K_{leaf} (Fig. 3). Further, as predicted from theory, the coordination of gas exchange and hydraulics was modulated by climate (Supplementary Appendix 1), as seen by the

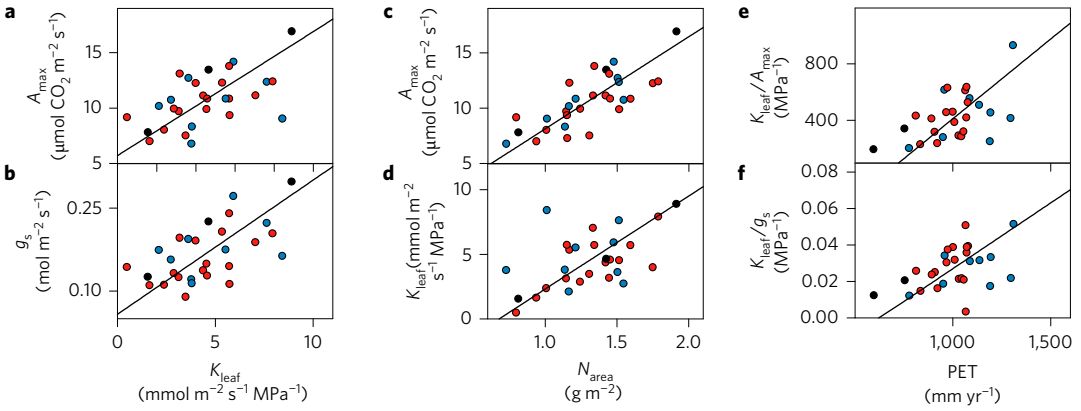

Figure 3 | Testing hydraulic theory in an evolutionary context across *Viburnum* species. a,**b**, Coordination of light-saturated CO_2 assimilation rate (A_{max}) (**a**) and stomatal conductance (g_s; **b**) with leaf hydraulic conductance (K_{leaf}) at leaf water potential of –0.3 MPa. **c**,**d**, Impact of nitrogen per unit leaf area (N_{area}) on A_{max} (**c**) and K_{leaf} (**d**). **e**,**f**, Coordination of native range potential evapotranspiration (PET) with hydraulic conductance to photosynthesis ratio (K_{leaf}/A_{max}) (**e**) and the hydraulic–stomatal conductance ratio (K_{leaf}/g_s) (**f**) across *Viburnum* species. The regression was obtained from fitted standardized major axes through the ahistorical data. Regression coefficients for the phylogenetic independent contrasts (not shown) obtained from the best fit evolutionary model (see Methods) are as follows: A_{max} versus K_{leaf}, $r = 0.53$ and $P = 0.002$; g_s versus K_{leaf}, $r = 0.42$ and $P = 0.015$; A_{max} versus N_{area}, $r = 0.57$ and $P < 0.001$; K_{leaf} versus N_{area}, $r = 0.26$ and $P = 0.003$; K_{leaf}/A_{max} versus PET, $r = 0.37$ and $P = 0.03$; K_{leaf}/g_s versus PET, $r = 0.39$ and $P = 0.02$. The regressions were obtained by fitting standardized major axes through the ahistorical data. Blue, red and black symbols represent, respectively, North American, Asian and European species.

tight correlations of K_{leaf} with $g_s \times$ potential evapotranspiration (PET) and $A_{max} \times$ PET (Supplementary Fig. 1 and Supplementary Tables 2 and 3) and the positive correlations of the hydraulic–stomatal conductance ratio (K_{leaf}/g_s) and the hydraulic conductance–photosynthetic rate ratio (K_{leaf}/A_{max}) with mean annual temperature (MAT; Supplementary Table 4) and PET across species (Fig. 3).

Across species, there was strong diversification in the partitioning of hydraulic resistance throughout the leaf. The percentage of hydraulic resistance distributed in the petiole, the major and minor veins, and outside-xylem pathways (i.e. through the bundle sheath and mesophyll) varied respectively from 0.9 to 50% (22% on average), 1.8 to 36% (13%), 0.3 to 12% (5%) and 22 to 97% (58%) (Supplementary Table 2). For a subset of species spanning the phylogeny, the leaf xylem hydraulic conductance (K_x) varied by fourfold and the outside-xylem conductance (K_{ox}) by 87-fold ($n = 17$ species; Supplementary Table 2). The high variation observed in the maximum K_{leaf} across species was very strongly correlated with K_{ox} and only weakly related to K_x (Fig. 4).

Gas exchange and hydraulics were associated with leaf size and venation architecture across the *Viburnum* species. Leaf size ranged from 19–149 cm^2 across species ($P < 0.001$, ANOVA, Supplementary Table 2), and both major and minor vein length per area varied by approximately twofold ($P < 0.001$ for both; ANOVA; Supplementary Table 2). K_{leaf} and its components, the hydraulic conductances of the leaf veins (K_v; not including the petiole xylem) and the outside xylem pathways (K_{ox}), and A_{max} were positively correlated with major VLA, and K_{leaf} and A_{max} were positively correlated with minor VLA (Fig. 5; $r = 0.35$–0.64; $P < 0.033$; Supplementary Tables 1–3). K_{leaf} and major VLA were negatively correlated with leaf size ($r = -0.37$ and -0.49 respectively, $P < 0.035$, Fig. 6; Supplementary Tables 1–3), consistent with the developmental coordination of leaf size and major VLA, by which larger leaves space their major veins further apart during expansion[34]. The hydraulic conductance in the major veins (K_{maj}) correlated positively with major VLA ($r = 0.66$, $P < 0.001$; Supplementary Tables 2–4). By contrast, no correlation was found between the hydraulic conductance in the minor veins (K_{min}) and minor VLA ($P = 0.88$). Finally, consistent with its strong dependence on vein density and on outside-xylem conductance, the maximum K_{leaf} was statistically independent of xylem traits

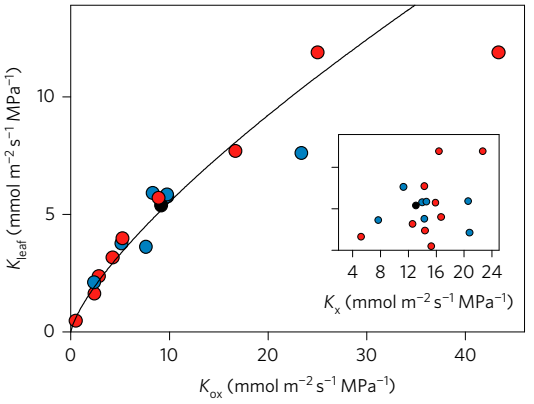

Figure 4 | Drivers of leaf hydraulic conductance for *Viburnum* species. Outside-xylem hydraulic conductance (K_{ox}) is the strongest driver of leaf hydraulic conductance (K_{leaf}), with little explanatory power across species, as shown in the inset, leaf xylem hydraulic conductance (K_x). The regression was obtained from fitted standardized major axes through the ahistorical data. Regression coefficients for the phylogenetic independent contrasts (not shown) obtained from the best fit evolutionary model (see Methods) are as follows: K_{leaf} versus K_{ox}, $r = 0.97$ and $P < 0.001$; K_{leaf} versus K_x, $r = 0.31$ and $P = 0.12$. Blue, red and black symbols represent, respectively, North American, Asian and European species.

within the veins, that is, the numbers and sizes of midrib xylem conduits, the theoretical midrib hydraulic conductance (K_t) (whether normalized by area, or midrib length per area), and the maximum conduit length ($P = 0.34$–0.86).

Discussion

Our results provide the first phylogenetic test of the theory for the evolutionary coordination of leaf hydraulics and gas exchange. The strong support shown for common garden-grown plants, within a phylogenetically well-resolved lineage establishes a key role for hydraulics in the evolution of photosynthetic rate. According to theory, a higher carbon uptake and stomatal conductance (A_{max} and g_s) should evolve in tight coordination

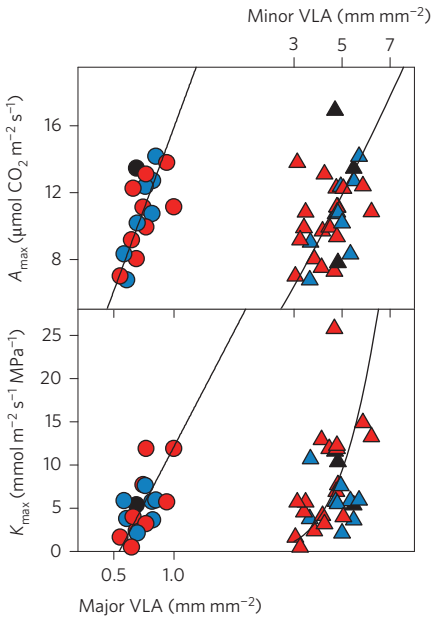

Figure 5 | Coordination of hydraulics and gas exchange with leaf venation. Both A_{max} (upper panel) and maximum K_{leaf} (K_{max}; lower panel) correlated with major vein length per area (major VLA, circles) and minor vein length per area (minor VLA, triangles). The regressions were obtained by fitting standardized major axes through the ahistorical data. Regression coefficients for the phylogenetic independent contrasts (not shown) obtained from the best fit evolutionary model (see Methods) were: A_{max} versus major VLA, $r = 0.50$ and $P = 0.025$; A_{max} versus minor VLA, $r = 0.36$ and $P = 0.033$; K_{leaf} versus major VLA, $r = 0.67$ and $P = 0.002$; K_{leaf} versus minor VLA, $r = 0.43$ and $P = 0.01$. Blue, red and black symbols represent, respectively, North American, Asian and European species.

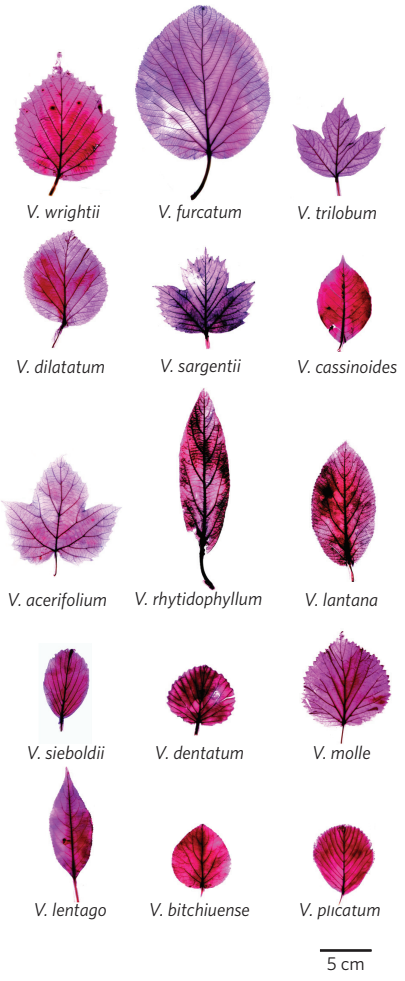

Figure 6 | Diversity of leaf size, shape and venation architecture in the model genus *Viburnum*. Chemically cleared leaves of 15 representative species are displayed from low to high leaf hydraulic conductance. Note that species with smaller leaves tend to have higher leaf hydraulic conductance values due to their higher VLA.

with a higher hydraulic supply (K_{leaf}), with their relationship modulated by climate variables, especially greater heat load and vapour pressure deficit (expected to relate to potential evapotranspiration, PET; Supplementary Appendix 1). Whereas high photosynthetic rates generally require proportionally higher N_{area}[15,35], a high K_{leaf} is also required to achieve high photosynthetic rates, and a disproportionately high K_{leaf} relative to g_s and A_{max} would be required in species that face higher evaporative demand to sustain a given operating leaf water potential[20,36,37]. We thus had expected correlations of K_{leaf} with $g_s \times$ PET (representing hydraulic demand) and $A_{max} \times$ PET (representing photosynthetic rate normalized for the effect of climate; Supplementary Appendix 1). We found strong support for model expectations, with species evolving a higher hydraulic supply relative to stomatal capacity in warmer habitats that would mitigate greater transpiration rates driven by higher vapour pressure deficit. The tight coordination observed was especially remarkable given that the common garden environment conditions differ from the native habitats for many of the species. Further, the coordination of leaf hydraulics with gas exchange is noteworthy, given that the stem and root architecture and hydraulics would also vary strongly across species; yet, this leaf-level coordination is consistent with the leaves representing a strong hydraulic bottleneck in the whole plant system[38]. Coordination of K_{leaf}, g_s and climate would enable the water potential gradient across the plant to be maintained within a relatively narrow range, irrespective of native habitat water availability and evaporative demand (Fig. 3 and Supplementary Appendix 1). Furthermore, our findings support the theory that the evolution of higher A_{max} necessitates an upwards shift in K_{leaf}, and/or that an upwards shift in K_{leaf} is an 'enabling trait' for an increase in A_{max}[7,39,40].

Increases in A_{max} and K_{leaf} would be selected for a higher relative growth rate when resource availability (higher irradiance, moisture or nutrient supply) is greater in the habitat or microhabitat, whereas decreases in A_{max} and K_{leaf} would be selected to reduce cost or increase efficiency when resource supplies are low[25,29,38]. In particular, we suspect that movements into different light environments may have driven the evolution of photosynthetic capacity in *Viburnum*, as previously shown for Hawaiian lobeliads[11]. Indeed, though measures of the native light environment do not exist for the species of *Viburnum* studied, A_{max} strongly correlated with maximum height for *Viburnum*, which can be used as a proxy for light environment given that maximum height tends to be ecologically correlated with high resource conditions[41], and especially irradiance for forest species (Supplementary Appendix 2). Thus, evolution into higher irradiance would have required the evolution of sufficient hydraulic capacity. Indeed, the coordination of K_{leaf} and gas exchange is especially evident in the Valvatotinus clade (spanning from *cassinoides* to *lantana* in Fig. 2), in which both A_{max} and K_{leaf} are elevated and show multiple complementary evolutionary shifts. The members of this clade possess one layer of elongated palisade cells[25] and they tend to have thicker leaves, both attributes characteristic of the open, well-lit environments these plants frequently occupy as adults[25].

Our results further provided important insights into the anatomical basis for the evolutionary diversification of leaf water transport. The diversification in K_{leaf} across *Viburnum* species was tightly linked with shifts in water transport properties and tissue anatomy outside the xylem. We found K_x was highly conserved relative to K_{ox}, and K_{ox} was the most important determinant of K_{leaf} across species. As previously proposed[29], diversification in K_{ox} as a means to shift K_{leaf} values is likely to be both more cost-effective and less developmentally constrained than shifts in K_x. Whereas shifts in K_x require modification of vein xylem traits, shifts in K_{ox} can be effected by multiple factors: (1) variation in VLA which would modify both the distance from xylem to the site of evaporation in the leaf and the bundle sheath surface area in the leaf, and thus significantly impact the resistance of water movement from the vein xylem to the mesophyll[33]; (2) variation in mesophyll anatomy; and/or (3) changes in aquaporin abundance and activity[42–45]. Indeed, the diversification of K_{ox} in *Viburnum* occurred alongside a parallel diversification in multiple structural features, including leaf size (Supplementary Table 2); leaf shape, with leaves ranging from entire to variously toothed and lobed (Fig. 6); mesophyll anatomy[25]; and venation architecture (Fig. 6). Both major and minor vein length per area were especially strong determinants of leaf hydraulic capacity and photosynthetic rate during evolutionary diversification in this lineage. The hydraulic importance of major vein length was further substantiated by hydraulic partitioning analysis in which major VLA correlated with the hydraulic conductance of the major veins. In contrast, no correlation was found between minor VLA and their hydraulic conductance. This independence is likely to arise at least in part from the tendency of species with lower minor VLA to have larger diameter minor veins, which would compensate for this variation, a relationship previously reported across 111 diverse vascular plants[46], and confirmed here for *Viburnum* ($r = -0.36$; $P < 0.035$, Supplementary Tables 1–3). The relationship of K_{ox} with major VLA is consistent with water exiting the vein system via third-order veins in addition to minor veins[47,48].

Conclusions

Across *Viburnum*, a phylogenetically well-resolved model lineage with highly diverse leaves, leaf water transport and gas exchange showed strongly coupled evolutionary diversification, driven by shifts in venation architecture and modulated by climate. These findings provide strong confirmation for a theory supporting a hydraulic basis for the evolution of the photosynthetic rate. The intrinsic requirement for hydraulic capacity to enable the evolution of high rates of photosynthesis has major implications. Just as hydraulic evolution has contributed to increases in the photosynthetic rate across major lineages throughout the history of plant life[1,32,49], it underlies the evolution of photosynthesis within individual lineages that diversified in leaf morphology, in climate, and in ecological niche. Our validation of a hydraulic basis for the evolution of a high photosynthetic rate provides key support for the proposal that hydraulic traits should be explicitly considered as underlying variables in determining species differences in photosynthetic rate, and as targets for improving crop plant productivity[50,51].

Methods

***Viburnum* phylogeny.** We used a well-supported *Viburnum* phylogeny for 80 species[25]. We focused on a subset of 30 species (Supplementary Table 2; Fig. 2) spanning most major clades within the tree[26] and growing in a common garden at the Arnold Arboretum of Harvard University (Jamaica Plain, MA, USA).

Leaf hydraulic conductance. In July 2010, mature, sun-exposed shoots from two to three individuals per species were collected in the Arnold Arboretum the day before measurements and placed in dark plastic bags filled with wet paper towels. They were transported directly to the laboratory at Brown University (Providence, RI, USA), where they were recut under ultra-pure water (Millipore Milli-Q Academic), by at least two nodes. They were then placed in buckets filled with ultra-pure water and covered in double dark plastic bags filled with wet paper towels to halt transpiration and enable the shoots to rehydrate overnight.

The next day, leaf hydraulic conductance was measured for three to eight leaves per individual per species (9–16 leaves per species) using the evaporative flux method[52]. Leaves were excised from shoots under ultra-pure water, parafilm was wrapped around their petiole and petioles were re-cut under water using a fresh razor blade. Petioles were sealed into compression fittings (Omnifit A2227 bore adaptor; Omnifit, Cambridge, UK) connected to a pressure-drop hydraulic flowmeter[53,54] that logged data every second to the computer to calculate flow rate (E). The flow solution was ultra-pure water degassed overnight with a vacuum pump and re-filtered (0.2 μm; syringe filter, Cole-Parmer, Vernon Hills, IL, USA). To ensure that the leaf was transpiring, it was held adaxial face up over a large box fan (Lakewood Engineering & Manufacturing Company, Chicago, IL, USA) and under floodlights (model 73828 1,000 W, 'UV filter'; Sears, Roebuck, Hoffman Estates, IL, USA) illuminating the leaf surface with >1,000 μmol m^{-2} s^{-1} photosynthetically active radiation. Leaf temperature was maintained between 23 and 28 °C by using a Pyrex container filled with water between the leaf and the floodlights. Leaves were allowed to transpire over the fan for at least 30 min and up to 4 h, until the E stabilized with a coefficient of variation <5% for at least 5 min, with no upwards or downwards trend. Measurements were discontinued if the flow suddenly changed, due to air bubbles, particles/mucilage blocking the flow of water, or stomatal closure. Leaf temperature was recorded once flow stabilized (before it was removed from the system), its petiole dabbed dry and immediately placed into a sealable bag (Whirl-Pack; Nasco, Fort Atkinson, WI, USA) with high humidity inside to halt transpiration. The leaf water potential driving force (Ψ_{leaf}) was measured after 30 min equilibration time in the bag using a pressure chamber (Plant Moisture Stress, Model 1000, Albany, OR, USA). K_{leaf} was calculated as $E/(-\Psi_{leaf})$ and further normalized by leaf area, obtained by measuring scanned images using ImageJ software[55] (http://imagej.nih.gov/ij/). To correct for the effect of water viscosity, K_{leaf} values were further standardized to 25 °C[56–58].

We accounted for the fact that for many species K_{leaf} can decline with leaf dehydration even at moderately negative water potentials[59,60]. We plotted K_{leaf} against the leaf water potential (Ψ_{leaf}) obtained at the end of the measurement, which in some cases reached values as low as −1.5 MPa, and we fitted linear functions to the data. In 16 out of 30 cases, the regression was significant ($P < 0.05$) and we calculated K_{max} as the intercept of the function fitted through the points[7], and estimated the K_{leaf} value at a reference water status within the realistic range of leaf transpiration, $\Psi_{leaf} = -0.3$ MPa ($K_{0.3MPa}$). For the 14 other species that did not show significant decline in K_{leaf} over the range of measured Ψ_{leaf}, K_{max} and $K_{0.3MPa}$ were calculated as the average of all K_{leaf} measurements[61–63]. We used $K_{0.3MPa}$ to test for correlation with gas exchange traits, and K_{max} to test for correlation with venation and other anatomical traits, following previous studies showing such relationships to be strongest for leaves at full turgor[7,19]. It is to be noted that no $K_{0.3MPa}$ is given for *Vibernum ichangense*, because the x-intercept of the linear regression of K_{leaf} with Ψ_{leaf} was greater than −0.3 MPa (Supplementary Table 2).

Partitioning of leaf hydraulic resistances inside and outside the xylem. We used the high-pressure flowmeter method (HPFM) to measure hydraulic conductance through the different vein orders on a subset of 17 *Viburnum* species, spanning the major lineages within the clade[28,29]. One to two leaves per two to three individuals per species were excised under water from the rehydrated shoots, and petioles wrapped with parafilm before they were re-cut under water using a fresh razor blade. Leaves were connected to the HPFM via a compression fitting. Pressurized degassed and re-filtered flow solution (0.5–0.6 MPa) was forced through a system of silicone and high-resistance tubing (PEEK; 0.125 mm internal diameter; Upchurch Scientific, Oak Harbor, WA, USA) before entering the leaf. The hydraulic conductance was calculated using pressure transducers (Omega PX-180; Omega Engineering, Stamford, CT, USA) before (P_1) and after (P_2) PEEK tubing of known resistance (R_{PT}), as $(P_1 - P_2)/(P_2 \times R_{PT})$. R_{PT} was obtained from the slope of the delivery pressure versus flow rate measured using an analytical balance (model XS205, ±10 μg sensitivity; Mettler Toledo, Columbus, OH, USA) and standardized to 25 °C to correct for the effect of viscosity of water through the tubing[56–58].

To determine the hydraulic resistance of the leaf xylem (R_x), we first applied 1–2 mm wide cuts to the minor vein system using a scalpel, by cutting between approximately 95% of tertiary veins in the leaf, taking care to avoid cutting any major veins (1°, 2° and 3°), resulting in 4–22 cuts per cm^2. Cuts were made until flow rate no longer increased. We note that much work has been done to validate the technique of cutting minor veins until the K_x no longer increases with additional minor vein cuts[28,64,65]. Indeed, vein cutting approaches to measuring maximum K_x values have been used for over a decade with the high-pressure flowmeter, and this technique has been validated against modelling approaches using a spatially explicit model of a leaf vein system, and against direct measurements of the vascular pressure using a pressure probe[30]. Measurements were logged onto the computer every 1 s, and once the flow stabilized with a coefficient of variation <5% for at least 5 min with no upwards or downwards trend, the hydraulic conductance was recorded, along with the temperature of the water flowing through the system, to correct for the viscosity effect on the resistance of the tubing and of the leaf. To determine the

hydraulic resistance of the minor veins, we applied central cuts to all tertiary veins in the lamina, and measured the resistance (R_{3o}) as $R_{min} = R_x - R_{3o}$. To determine the hydraulic resistance of the petiole (R_{pet}), the lamina was excised and the resistance measured. At the end of the petiole hydraulic conductance measurement, a leak test was conducted by sealing the petiole end with super glue (Loctite 409 Glue; McMaster-Carr, Los Angeles, CA, USA) and accelerator (Loctite 712 accelerator), and hydraulic conductance was measured. Small leaks occurred in 19 out of 63 measurements, and were subtracted from the measured conductances. Leaf area was measured at the end of the measurements using a flatbed scanner and calculated in ImageJ[55] (http://imagej.nih.gov/ij/). All resistances were then normalized by leaf size. The hydraulic resistance of the major veins (R_{maj}) was obtained as $R_{maj} = R_{3o} - R_{pet}$. We obtained the outside-xylem hydraulic resistance using the formula $R_{ox} = (1/K_{max}) - R_x$, using K_{max} values obtained for the same plants with the evaporative flux method (EFM, see the section above), The percentage of hydraulic resistances in the xylem (%R_x), outside-xylem (%R_{ox}), minor veins (%R_{min}), major veins (%R_{maj}) and petiole (%R_{pet}) were obtained by dividing their given resistances by total leaf hydraulic resistance ($1/K_{max}$). The hydraulic conductance of the xylem (K_x) was obtained as $1/R_x$ and K_{ox} was obtained as $1/((1/K_{max}) - (1/K_x))$.

Measurement of foliar gas exchange and nitrogen concentration. Mean values for light-saturated CO_2 assimilation rate (A_{max}) were the previously published values for the same plants of the 30 *Viburnum* species grown at the Arnold Arboretum[25]. Briefly, for each species, A_{max} was measured on several sun-exposed mature leaves of several individuals using a LiCOR 6400XT (Li-COR Biosciences, Lincoln, NB, USA) between 10:00 a.m. and 2:00 p.m., at an irradiance of 1,500 mmol m^{-2} s^{-1}, 400 ppm of CO_2 partial pressure and a relative humidity ranging from 30 to 50%. At the same time as the A_{max} measurements were taken, the stomatal conductances (g_s, mmol H_2O m^{-2} s^{-1}) were also recorded. Nitrogen per leaf area was determined on a 1,000 µg dry-matter aliquot using a Carbon–Nitrogen Elemental Analyser (CE Instruments model INC 2100; CE Elantech Inc., Lakewood, NJ, USA); data were used as previously published for the same individuals[16].

Leaf area and vein architecture. For each species, leaf area (LA) was obtained by collecting 13 to 20 sun-exposed mature leaves from several individuals between 2009 and 2010. Each leaf was photographed individually and leaf areas were measured using ImageJ.

Minor VLA and diameter were measured for all 30 *Viburnum* species. For each species, central 2 × 3 cm^2 pieces were cut from one sun-exposed mature leaf from each of three individuals and cleared with sodium hydroxide followed by sodium hypochlorite on a hot plate[66]. Each leaf piece included all vein orders except for the primary vein. Veins were stained with Safranin O and digital images representing 7 mm^2 of leaf area were captured with a Nikon DXM1200C digital camera coupled to a Nikon Eclipse E600 (Nikon, Melville, NY, USA) compound light microscope. From the digital images, the total length of the minor veins (fourth vein order and above) was measured with ImageJ and VLA was calculated. One vein diameter per minor vein order per image was measured with ImageJ, and these were averaged.

For the 17 species selected for hydraulic partitioning, we cleared whole leaves to additionally characterize the major venation. Three leaves from two to three individuals per species were chemically cleared in 5% NaOH solution and bleach following standard procedures[66] and scanned (using a flatbed scanner; Epson Perfection 4490 Photo Scanner, CA, USA; 1,200 pixels per inch). Major VLA (mm mm^{-2}) was measured using ImageJ[66].

Leaf xylem anatomy. To characterize the midrib xylem anatomy, we measured major and minor axis diameters of all xylem conduits in the midrib from three leaves of two to three individuals of each of the 17 selected species measured for leaf hydraulic partitioning. The total number of conduits and maximum conduit diameter were averaged across the midribs of the three sections. We determined the theoretical midrib conductivity by treating each conduit as an ellipse and using Poiseuille's equation modified for ellipses[30,67],

$$K_t = \sum \frac{\pi a^3 b^3}{64\eta(a^2 + b^2)} \quad (2)$$

where a and b are the major and minor axes of the ellipse and η is water viscosity at 25 °C. Theoretical hydraulic conductance normalized by leaf area was calculated by dividing K_t by LA, and theoretical hydraulic conductance normalized by midrib length and leaf area was calculated as K_t/(LA × midrib length).

We measured maximum vessel length for 21 species (Supplementary Table 2, column AA) by selecting three to six leaves from shoots of the different individuals that had been rehydrated overnight. Leaves were connected by silicone tubing to a four-way valve connected to a syringe. Zip ties were applied around the tubing and petiole to ensure a tight seal. Air pressure was applied using a caulking gun while the leaf was placed under water, under a light source. Using a scalpel, cuts were made throughout the leaf beginning with the highest order veins, and progressively to lower order veins, and finally along the midrib towards the leaf base, until air bubbles first emerged from the xylem, indicating maximum conduit length. Maximum vessel length from the petiole to leaf veins also varied strongly across species, i.e. conduits ended in the midrib in two species and in the minor veins in one, with the majority of the tested species having their longest vessels ending in the secondary veins (14 out of 21) (Supplementary Table 2).

Statistical and phylogenetic comparative analyses. We tested differences in traits among species using one-way analyses of variance (ANOVAs; Minitab Release 16). All data were log-transformed to improve normality and heteroscedasticity[68]. To test for variation across K_{leaf} values measured with the EFM, we performed a one-way ANOVA on log-transformed data, with mean leaf water potential (Ψ_{leaf}) as a covariate, to control for the decline of K_{leaf} with Ψ_{leaf} during measurements.

We examined 32 hypotheses relating leaf hydraulics to physiology, climate, anatomy and leaf venation (Supplementary Table 2). To examine the evolutionary dynamics of leaf traits and correlations among traits, we utilized the phylogenetic analyses from ref. 25, with trees pruned to include only the taxa sampled in this study. Ancestral character states at all internal nodes were inferred for A_{max} and K_{leaf} using maximum likelihood[69,70]. To test whether two traits were correlated in their evolution, we first evaluated the fit of different models of trait evolution. We compared a Brownian motion (BM) model and multiple Ornstein–Uhlenbeck (OU) models[71]: an OU model with a single optimum (OU1) and an OU model that fit two separate optima, one for the Valvatinotinus clade and one for all other *Viburnum* (OU2). The best fitting model for each trait was chosen using the Akaike Information Criterion corrected for low number of samples (n). We then tested for correlated evolution between traits by calculating phylogenetic independent contrasts for each trait with the appropriate tree transformation (BM, OU1 or OU2) and performed linear regression between contrasts for 32 correlations. When initial non-phylogenetic regressions indicated that relationships were nonlinear, the evolutionary relationships were evaluated on log-transformed data. Primary analyses were performed using the Bayesian maximum clade credibility phylogeny, with molecular branch lengths smoothed ultrametrically and a root age set to one[25].

To test the influence of branch lengths and uncertainty in tree topology on our inferences of character evolution, we repeated these analyses across 200 alternate trees sampled from the posterior probability distribution. We created three sets of the 200 trees with different branch lengths: all branches equal to 1 (Brl1), an ultrametric tree smoothed with the root set to 1 (UM) or untransformed, i.e. with molecular branch lengths (MolBrl). For each set of 200 trees (Brl1, UM and MolBrl), we ran the analyses as described above. For each correlation, and for each evolutionary model (BM, OU), the percentage of significant p values was calculated for each set of trees (Brl1, UM, MolBrl; Supplementary Fig. 2). All phylogenetic comparative analyses were performed in R version 3.1.1 using the packages APE[72], GEIGER[73] and OUCH[71,74].

To control for multiple comparisons, we performed a false detection rate analysis on the 32 tested hypotheses[75]. We found the minimum level for significance taking into account multiple testing was of $p = 0.035$ (see Supplementary Table 5 for the false detection rate calculator).

Determination of climate variables. To determine climate variables for the species in this study we downloaded georeferenced occurrences from the Global Biodiversity Information Facility (GBIF; http://www.gbif.org). For 23 of our taxa we used data previously published[24]. For an additional six species included in this study, we downloaded data with the 'basis of record' field constrained to 'specimen', and combined these data with the previously published data[24]. No coordinates were available for *Viburnum lantana var. discolor*. Following latest protocols[24], we first excluded coordinates that appeared outside the natural geographical range of *Viburnum* and thus represented cultivated material, and further cleansed the coordinates according to a recently developed protocol[76], removing coordinates that were overly imprecise (i.e. records that have coordinates to only the first decimal), as well as coordinates that match to political centroids (i.e. coordinates that would refer to the centre of countries or states, which are used when herbarium data or unknown exact locations are entered in GBIF). Using this reduced dataset, mean annual temperature (MAT) and precipitation (MAP) were obtained for each locality from the WordClim – Global Climate Data website[77] (http://www.worldclim.org/) using a 2.5 arc-minute resolution from the generic grids and the R raster package[78]. From the CGIAR-CSI database, we obtained annual evapotranspiration (PET) and the aridity index (AI = MAP/PET), which are calculated using the WorldClim data.

Received 4 December 2015; accepted 22 April 2016; published 27 May 2016

References

1. Sperry, J. S. Evolution of water transport and xylem structure. *Int. J. Plant Sci.* **164,** S115–S127 (2003).
2. Cowan, I. R. & Farquhar, G. D. Stomatal function in relation to leaf metabolism and environment. **31,** 471–505 (1977).
3. Givnish, T. J. & Vermeij, G. J. Sizes and shapes of liane leaves. *Am. Nat.* **110,** 743–778 (1976).
4. Givnish, T. J. (ed.) *On the Economy of Plant Form and Function* (Cambridge Univ. Press, 1986).

5. Brodribb, T. J. & Feild, T. S. Stem hydraulic supply is linked to leaf photosynthetic capacity: evidence from New Caledonian and Tasmanian rainforests. *Plant Cell Environ.* **23,** 1381–1388 (2000).
6. Brodribb, T. J., Holbrook, N. M., Zwieniecki, M. A. & Palma, B. Leaf hydraulic capacity in ferns, conifers and angiosperms: impacts on photosynthetic maxima. *New Phytol.* **165,** 839–846 (2005).
7. Brodribb, T. J., Feild, T. S. & Jordan, G. J. Leaf maximum photosynthetic rate and venation are linked by hydraulics. *Plant Physiol.* **144,** 1890–1898 (2007).
8. Feild, T. S. & Balun, L. Xylem hydraulic and photosynthetic function of *Gnetum* (Gnetales) species from Papua New Guinea. *New Phytol.* **177,** 665–675 (2008).
9. Sack, L. & Frole, K. Leaf structural diversity is related to hydraulic capacity in tropical rain forest trees. *Ecology* **87,** 483–491 (2006).
10. Fiorin, L., Brodribb, T. J. & Anfodillo, T. Transport efficiency through uniformity: organization of veins and stomata in angiosperm leaves. *New Phytol.* **209,** 216–227 (2016).
11. Givnish, T. J., Montgomery, R. A. & Goldstein, G. Adaptive radiation of photosynthetic physiology in the Hawaiian lobeliads: light regimes, static light responses, and whole-plant compensation points. *Am. J. Bot.* **91,** 228–246 (2004).
12. Pittermann, J. *et al.* The relationships between xylem safety and hydraulic efficiency in the cupressaceae: the evolution of pit membrane form and function. *Plant Physiol.* **153,** 1919–1931 (2010).
13. Gleason, S. M. *et al.* Weak tradeoff between xylem safety and xylem-specific hydraulic efficiency across the world's woody plant species. *New Phytol.* **209,** 123–136 (2016).
14. Mason, C. M. & Donovan, L. A. Evolution of the leaf economics spectrum in herbs: evidence from environmental divergences in leaf physiology across *Helianthus* (Asteraceae). *Evolution* **69,** 2705–2720 (2015).
15. Wright, I. J. *et al.* The worldwide leaf economics spectrum. *Nature* **428,** 821–827 (2004).
16. Edwards, E. J., Chatelet, D. S., Sack, L. & Donoghue, M. J. Leaf life span and the leaf economic spectrum in the context of whole plant architecture. *J. Ecol.* **102,** 328–336 (2014).
17. Edwards, E. J. Correlated evolution of stem and leaf hydraulic traits in *Pereskia* (Cactaceae). *New Phytol.* **172,** 479–489 (2006).
18. Liu, H. *et al.* Strong phylogenetic signals and phylogenetic niche conservatism in ecophysiological traits across divergent lineages of Magnoliaceae. *Sci. Rep.* **5,** 12246 (2015).
19. Sack, L., Cowan, P. D., Jaikumar, N. & Holbrook, N. M. The 'hydrology' of leaves: co-ordination of structure and function in temperate woody species. *Plant Cell Environ.* **26,** 1343–1356 (2003).
20. Brodribb, T. J. & Jordan, G. J. Internal coordination between hydraulics and stomatal control in leaves. *Plant Cell Environ.* **31,** 1557–1564 (2008).
21. Scoffoni, C. *et al.* Light-induced plasticity in leaf hydraulics, venation, anatomy and gas exchange in ecologically diverse Hawaiian lobeliads. *New Phytol.* **207,** 43–58 (2015).
22. Damour, G., Simonneau, T., Cochard, H. & Urban, L. An overview of models of stomatal conductance at the leaf level. *Plant Cell Environ.* **33,** 1419–1438 (2010).
23. Wong, S. C., Cowan, I. R. & Farquhar, G. D. Stomatal conductance correlates with photosynthetic capacity. *Nature* **282,** 424–426 (1979).
24. Schmerler, S. B. *et al.* Evolution of leaf form correlates with tropical-temperate transitions in *Viburnum* (Adoxaceae). *Proc. R. Soc. B* **279,** 3905–3913 (2012).
25. Chatelet, D. S., Clement, W. L., Sack, L., Donoghue, M. J. & Edwards, E. J. The evolution of photosynthetic anatomy in *Viburnum* (Adoxaceae). *Int. J. Plant Sci.* **174,** 1277–1291 (2013).
26. Clement, W. L., Arakaki, M., Sweeney, P. W., Edwards, E. J. & Donoghue, M. J. A chloroplast tree for *Viburnum* (Adoxaceae) and its implications for phylogenetic classification and character evolution. *Am. J. Bot.* **101,** 1029–1049 (2014).
27. Spriggs, E. L. *et al.* Temperate radiations and dying embers of a tropical past: the diversification of *Viburnum*. *New Phytol.* **207,** 340–354 (2015).
28. Sack, L., Streeter, C. M. & Holbrook, N. M. Hydraulic analysis of water flow through leaves of sugar maple and red oak. *Plant Physiol.* **134,** 1824–1833 (2004).
29. Sack, L., Tyree, M. T. & Holbrook, N. M. Leaf hydraulic architecture correlates with regeneration irradiance in tropical rainforest trees. *New Phytol.* **167,** 403–413 (2005).
30. Cochard, H., Nardini, A. & Coll, L. Hydraulic architecture of leaf blades: where is the main resistance? *Plant Cell Environ.* **27,** 1257–1267 (2004).
31. Sommerville, K. E., Sack, L. & Ball, M. C. Hydraulic conductance of *Acacia phyllodes* (foliage) is driven by primary nerve (vein) conductance and density. *Plant Cell Environ.* **35,** 158–168 (2012).
32. Sack, L. & Scoffoni, C. Leaf venation: structure, function, development, evolution, ecology and applications in past, present and future. *New Phytol.* **198,** 938–1000 (2013).
33. Buckley, T. N., John, G. P., Scoffoni, C. & Sack, L. How does leaf anatomy influence water transport outside the xylem? *Plant Physiol.* **168,** 1616–1635 (2015).
34. Sack, L. *et al.* Developmentally-based scaling of leaf venation architecture explains global ecological patterns. *Nature Commun.* **3,** 837 (2012).
35. Field, C. & Mooney, H. A. in *On the Economy of Plant Form and Function* (ed. Givnish, T. J.) 25–56 (Cambridge Univ. Press, 1986).
36. Osborne, C. P. & Sack, L. Evolution of C-4 plants: a new hypothesis for an interaction of CO_2 and water relations mediated by plant hydraulics. *Phil. Trans. R. Soc. B* **367,** 583–600 (2012).
37. Cornwell, W. K., Bhaskar, R., Sack, L., Cordell, S. & Lunch, C. K. Adjustment of structure and function of Hawaiian *Metrosideros polymorpha* at high vs. low precipitation. *Funct. Ecol.* **21,** 1063–1071 (2007).
38. Sack, L. & Holbrook, N. M. Leaf hydraulics. *Annu. Rev. Plant Biol.* **57,** 361–381 (2006).
39. Donoghue, M. J. Key innovations, convergence, and success: macroevolutionary lessons from plant phylogeny. *Paleobiology* **31,** 77–93 (2005).
40. Edwards, E. J. & Donoghue, M. J. Is it easy to move and easy to evolve? Evolutionary accessibility and adaptation. *J. Exp. Bot.* **64,** 4047–4052 (2013).
41. Thomas, S. C. & Bazzaz, F. A. Asymptotic height as a predictor of photosynthetic characteristics in Malaysian rain forest trees. *Ecology* **80,** 1607–1622 (1999).
42. Noblin, X. *et al.* Optimal vein density in artificial and real leaves. *Proc. Natl. Acad. Sci. USA* **105,** 9140–9144 (2008).
43. Flexas, J., Scoffoni, C., Gago, J. & Sack, L. Leaf mesophyll conductance and leaf hydraulic conductance: an introduction to their measurement and coordination. *J. Exp. Bot.* **64,** 3965–3981 (2013).
44. Buckley, T. N. The contributions of apoplastic, symplastic and gas phase pathways for water transport outside the bundle sheath in leaves. *Plant Cell Environ.* **38,** 7–22 (2015).
45. Kim, Y. X. & Steudle, E. Light and turgor affect the water permeability (aquaporins) of parenchyma cells in the midrib of leaves of *Zea mays*. *J. Exp. Bot.* **58,** 4119–4129 (2007).
46. Feild, T. S. & Brodribb, T. J. Hydraulic tuning of vein cell microstructure in the evolution of angiosperm venation networks. *New Phytol.* **199,** 720–726 (2013).
47. Nardini, A. & Salleo, S. Effects of the experimental blockage of the major veins on hydraulics and gas exchange of *Prunus laurocerasus* L. leaves. *J. Exp. Bot.* **54,** 1213–1219 (2003).
48. Zwieniecki, M. A., Melcher, P. J., Boyce, C. K., Sack, L. & Holbrook, N. M. Hydraulic architecture of leaf venation in *Laurus nobilis* L. *Plant Cell Environ.* **25,** 1445–1450 (2002).
49. Brodribb, T. J. & Feild, T. S. Leaf hydraulic evolution led a surge in leaf photosynthetic capacity during early angiosperm diversification. *Ecol. Lett.* **13,** 175–183 (2010).
50. Brodribb, T. J., Holloway-Phillips, M.-M. & Bramley, H. *Crop Physiology: Applications for Genetic Improvement and Agronomy* 2nd edn (Oxford Academy Press, 2015).
51. Sack, L. *et al.* Plant water transport as a central hub from plant to ecosystem function: meeting report for "Emerging Frontiers in Plant Hydraulics" (Washington, DC, 2015). *Plant Cell Environ.* (in the press).
52. Sack, L. & Scoffoni, C. Measurement of leaf hydraulic conductance and stomatal conductance and their responses to irradiance and dehydration using the evaporative flux methods (EFM). *J. Visual. Exp.* **e4179,** 1–7 (2012).
53. Brodribb, T. J. & Cochard, H. Hydraulic failure defines the recovery and point of death in water-stressed conifers. *Plant Physiol.* **149,** 575–584 (2009).
54. Sack, L., Bartlett, M., Creese, C., Guyot, G. & Scoffoni, C. *Constructing and Operating a Hydraulics Flow Meter* (Prometheus Wiki, 2011); http://prometheuswiki.publish.csiro.au/tiki-index.php?page=Constructing+and+operatinga+hydraulics+flow+meter
55. Abramoff, M. D., Magalhaes, P. J. & Ram, S. J. Image processing with ImageJ. *Biophoton. Int.* **11** 36–42 (2004).
56. Weast, R. C. *Handbook of Chemistry and Physics* 54th edn (CRC Press, 1974).
57. Yang, S. D. & Tyree, M. T. Hydraulic resistance in *Acer saccharum* shoots and its influence on leaf water potential and transpiration. *Tree Physiol.* **12,** 231–242 (1993).
58. Sack, L., Melcher, P. J., Zwieniecki, M. A. & Holbrook, N. M. The hydraulic conductance of the angiosperm leaf lamina: a comparison of three measurement methods. *J. Exp. Bot.* **53,** 2177–2184 (2002).
59. Brodribb, T. J. & Holbrook, N. M. Stomatal closure during leaf dehydration, correlation with other leaf physiological traits. *Plant Physiol.* **132,** 2166–2173 (2003).
60. Scoffoni, C., McKown, A. D., Rawls, M. & Sack, L. Dynamics of leaf hydraulic conductance with water status: quantification and analysis of species differences under steady-state. *J. Exp. Bot.* **63,** 643–658 (2012).
61. Scoffoni, C., Pou, A., Aasamaa, K. & Sack, L. The rapid light response of leaf hydraulic conductance: new evidence from two experimental methods. *Plant Cell Environ.* **31,** 1803–1812 (2008).
62. Brodribb, T. J. & Holbrook, N. M. Changes in leaf hydraulic conductance during leaf shedding in seasonally dry tropical forest. *New Phytol.* **158,** 295–303 (2003).
63. Nardini, A., Pedà, G. & La Rocca, N. Trade-offs between leaf hydraulic capacity and drought vulnerability: morpho-anatomical bases, carbon costs and ecological consequences. *New Phytol.* **196,** 788–798 (2012).
64. Nardini, A., Gortan, E. & Salleo, S. Hydraulic efficiency of the leaf venation system in sun- and shade-adapted species. *Funct. Plant Biol.* **32,** 953–961 (2005).

65. Nardini, A., Raimondo, F., Lo Gullo, M. A. & Salleo, S. Leafminers help us understand leaf hydraulic design. *Plant Cell Environ.* **33,** 1091–1100 (2010)
66. Scoffoni, C., Sack, L. & contributors *Quantifying Leaf Vein Traits* (Prometheus Wiki, 2013); http://prometheuswiki.publish.csiro.au/tiki-index.php?page=Quantifying+leaf+vein+traits
67. Lewis, A. M. & Boose, E. R. Estimating volume flow-rates through xylem conduits. *Am. J. Bot.* **82,** 1112–1116 (1995).
68. Sokal, R. R. & Rohlf, F. J. *Biometry: the Principles and Practice of Statistics in Biological Research* 3rd edn (W. H. Freeman and Company, 1995).
69. Pagel, M. Detecting correlated evolution on phylogenies - a general method for the comparative analysis of discrete characters. *Proc. R. Soc. B* **255,** 37–45 (1994).
70. Pagel, M. The maximum likelihood approach to reconstructing ancestral character states of discrete characters on phylogenies. *Systematic Biology* **48,** 612–622 (1999).
71. Butler, M. A. & King, A. A. Phylogenetic comparative analysis: a modeling approach for adaptive evolution. *Am. Nat.* **164,** 683–695 (2004).
72. Paradis, E., Claude, J. & Strimmer, K. APE: analyses of phylogenetics and evolution in R language. *Bioinformatics* **20,** 289–290 (2004).
73. Harmon, L. J., Weir, J. T., Brock, C. D., Glor, R. E. & Challenger, W. GEIGER: investigating evolutionary radiations. *Bioinformatics* **24,** 129–131 (2008).
74. King, A. A. & Butler, M. A. *OUCH: Ornstein-Uhlenbeck Models for Phylogenetic Comparative Hypotheses (R Package)* (CRAN, 2009); http://ouch.r-forge.r-project.org
75. Benjamini, Y. & Hochberg, Y. Controlling the false discovery rate: a practical and powerful approach to multiple testing. *J. R. Stat. Soc. B* **57,** 289–300 (1995).
76. Edwards, E. J., De Vos, J. & Donoghue, M. J. Brief Communications Arising: doubtful pathways to cold tolerance in plants. *Nature* **521,** E6–E7 (2015).
77. Humans, R. J., Cameron, S. E., Parra, J. L., Jones, P. G. & Jarvis, A. Very high resolution interpolated climate surfaces for global land areas. *Int. J. Climatol.* **25,** 1965–1978 (2005).
78. Humans, R. J. *RASTER: Geographic Data Analysis and Modeling. R Package Version 2.3-33* (CRAN, 2015); http://CRAN.R-project.org/package=raster

Acknowledgements

We thank the staff at the Arnold Arboretum of Harvard University, Erin Riordan for help with climate data, and M. Alfaro, M. Bartlett, M. Caringella, J. Chang and G. John for helpful comments on the manuscript. We would like to thank T. Givnish and two anonymous reviewers for their constructive comments. This work was funded by the Department of Ecology and Evolutionary Biology at UCLA, a UCLA Dissertation Year Fellowship and NSF grants IOS-0842771 to L.S., IOS-0843231 to E.J.E., and IOS-0842800 to M.J.D.

Author contributions

C.S., D.S.C., M.J.D., E.J.E. and L.S. designed experiments. C.S., D.S.C., J.P.K. and M.R. performed experiments. C.S. and D.S.C. analysed data. C.S. and L.S. wrote the paper with inputs from all authors.

Additional information

Supplementary information is available online. Reprints and permissions information is available online at www.nature.com/reprints. Correspondence and requests for materials should be addressed to C.S.

Competing interests

The authors declare no competing financial interests